Check for updates

Received: 23 October 2023 | Revised: 21 March 2024 | Accepted: 22 March 2024

DOI: 10.1111/psyp.14582

PSYCHOPHYSIOLOGY SPR WILEY

ORIGINAL ARTICLE

A new method for tracking the preparatory activation of target templates for visual search with high temporal precision

Gordon Dodwell | **Rebecca Nako** | **Martin Eimer**

School of Psychological Sciences, Birkbeck, University of London, London, UK

Correspondence
Gordon Dodwell, School of Psychological Sciences, Birkbeck, University of London, Malet Street, London WC1E 7HX, UK.
Email: g.dodwell@bbk.ac.uk; gcdodwell@gmail.com

Funding information
Economic and Social Research Council, Grant/Award Number: ES/V002708/1

Abstract

Efficiently selecting task-relevant objects during visual search depends on foreknowledge of their defining characteristics, which are represented within attentional templates. These templates bias attentional processing toward template-matching sensory signals and are assumed to become anticipatorily activated prior to search display onset. However, a direct neural signal for such preparatory template activation processes has so far remained elusive. Here, we introduce a new *high-definition rapid serial probe presentation* paradigm (RSPP–HD), which facilitates high temporal resolution tracking of target template activation processes in real time via monitoring of the N2pc component. In the RSPP–HD procedure, task-irrelevant probe displays are presented in rapid succession throughout the period between task-relevant search displays. The probe and search displays are homologously formed by lateralized "clouds" of colored dots, yielding probes that occur at task-relevant locations without confounding template-guided and salience-driven attentional shifts. Target color probes appearing at times when a corresponding target template is active should attract attention, thereby eliciting an N2pc. In a condition where new probe displays appeared every 50 ms, probe N2pcs were reliably elicited during the final 800 ms prior to search display onset, increasing in amplitude toward the end of this preparation period. Analogous temporal profiles were also observed with longer intervals between probes. These findings show that search template activation processes are transient and that their temporal profile can be reliably monitored at high-sampling frequencies with the RSPP–HD paradigm. This procedure offers a new route to approach various questions regarding the content and temporal dynamics of attentional control processes.

KEYWORDS

attentional control, attentional templates, event-related brain potentials (ERP), N2pc component, visual search

This is an open access article under the terms of the Creative Commons Attribution License, which permits use, distribution and reproduction in any medium, provided the original work is properly cited.
© 2024 The Authors. *Psychophysiology* published by Wiley Periodicals LLC on behalf of Society for Psychophysiological Research.

1 | INTRODUCTION

In visual search, the successful detection of target objects depends on knowledge of their unique attributes. Internal representations of these defining characteristics, known as "attentional templates," bias attentional processing toward sensory signals with template-matching features, thereby promoting adaptive top-down selectivity (Desimone & Duncan, 1995; Duncan, 2006; Duncan & Humphreys, 1989; Eimer, 2014; Giesbrecht et al., 2006; Huynh Cong & Kerzel, 2021; Ort & Olivers, 2020; Stokes et al., 2009; Wolfe, 2007, 2021). To proactively facilitate the detection and identification of target objects, target templates are assumed to be already activated during the preparation for search. However, no immediate neural signal for such preparatory search template activation processes has been discovered, so their existence remains elusive.

We recently developed a method (*rapid serial probe presentation* procedure, RSPP; Grubert & Eimer, 2018, 2019, 2020; Dodwell et al., 2024) to track search template activations in real time. Participants searched for color-defined targets, and each search display was preceded by a series of task-irrelevant circular probe displays containing a color singleton. These probes appeared at regular intervals between successive circular search displays, which contained a color-defined target among several nontarget objects in multiple different colors. Probe singletons that matched the target color triggered an N2pc component (an ERP marker of attentional allocation; see Eimer, 1996; Luck & Hillyard, 1994; Woodman & Luck, 1999), indicating that they attracted attention in a task-set contingent fashion (see Eimer & Kiss, 2008; Folk et al., 1992). In contrast, probe singletons in a nontarget color did not elicit any N2pcs. The presence of N2pc components to a particular target-color probe was interpreted as evidence that a corresponding target-color search template was activated during the time when this probe was presented. Importantly, these probe N2pcs only emerged during the later phase of the preparation period and were largest immediately prior to search display onset, suggesting that target-color templates were newly activated on each trial. In addition, the time point at which probe N2pcs first appeared was influenced by manipulations of the interval between successive search displays (Grubert & Eimer, 2018, Exp. 3). Specifically, probe N2pcs emerged 600 ms after the previous search display when the interval was consistently short (1000 ms), but only after 1600 ms when the interval was consistently longer (2600 ms). This finding demonstrates that the time course of target template activation is sensitive to temporal expectations regarding the arrival of the next task-relevant search display.

These initial observations provided an important first step toward demonstrating the existence and temporal profile of preparatory search templates. However, the particular probe presentation procedures employed in this work also have some serious limitations. Because probe displays only appeared every 200 ms, temporal sampling was relatively sparse, thus limiting the validity of claims about template activation dynamics within and across trials. It would clearly be desirable to probe search template activation more frequently during search periods. In addition, there are two other aspects of the probe techniques used which are problematic, because they may challenge the validity of linking probe-elicited N2pc components with the preparatory activation of color-specific search templates. On the one hand, the circular color singleton probe displays always appeared at different locations (closer to fixation) than the circular search displays. This was deemed necessary to prevent the probes from interfering with search display processing. However, the fact that they appeared at locations known to be task-irrelevant could have substantially reduced the ability of target-matching probes to attract attention. As a result, the true extent of template activation may have been seriously underestimated by measuring N2pc components to these probes. On the other hand, these target-matching probes were always color singletons. Because of their salience, they may have triggered some degree of task-independent bottom–up attentional capture. In this case, the N2pc components triggered by these probes would not have been exclusive markers of search template activation processes, and the pattern of N2pc results observed in our previous work may have thus overestimated the degree to which processes were activated during search preparation.

The goal of the current study was to address these issues by testing a new and improved method of probing preparatory search template activation. Here, we introduce a new high-definition RSPP paradigm (RSPP–HD), which was developed to address and resolve all three problematic issues inherent in the original singleton probe procedure, as noted above. With the RSPP–HD procedure, preparatory template activation can potentially be sampled in real time at considerably higher temporal resolutions. Moreover, it employs target-colored probes that are in no way more salient than any other element within the probe displays and are therefore no longer prone to triggering exogenous attentional capture. Finally, and perhaps most importantly, items in the probe and search displays now always occupy the same locations, thereby eliminating any concerns that the probes might attract reduced attention by appearing at task-irrelevant locations.

The general experimental setup is illustrated in Figure 1. Two "clouds" composed of colored dots were presented to the left and right of screen center at regular

14698986, 2024, 8, Downloaded from https://onlinelibrary.wiley.com/doi/10.1111/psyp.14582 by Test, Wiley Online Library on [08/07/2024]. See the Terms and Conditions (https://onlinelibrary.wiley.com/terms-and-conditions) on Wiley Online Library for rules of use; OA articles are governed by the applicable Creative Commons License

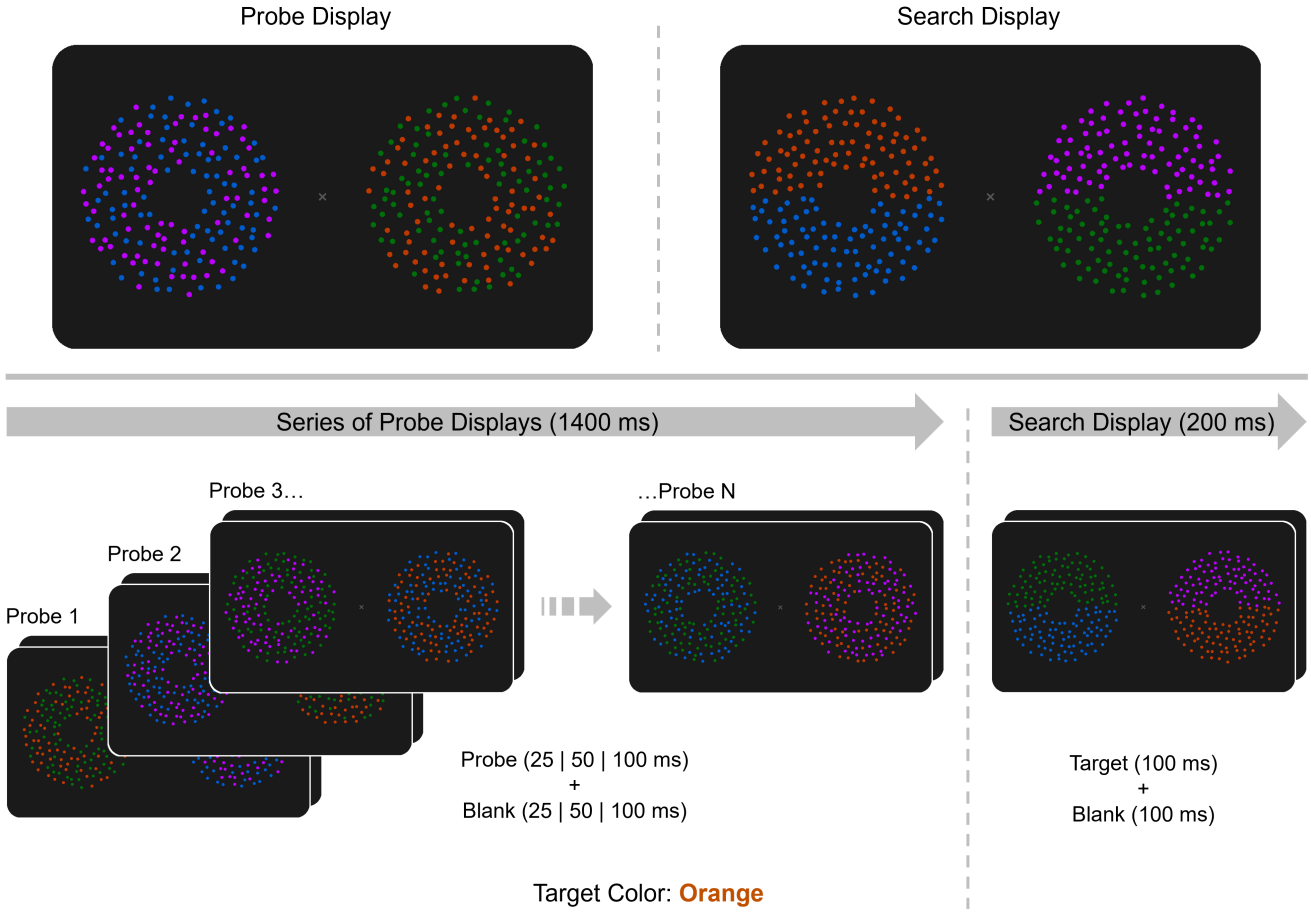

FIGURE 1 Probe and search displays of the HD-RSPP paradigm (top left, top right) with an example of the trial sequence (bottom). In probe displays, the dots within each cloud were pseudo-randomly colored to avoid producing any discernible shape or pattern. In search displays, the dots within the top and bottom halves of each cloud were uniformly colored, producing a discernibly "split" structure. Trials included 28, 14, and 7 probe displays (*N*) in the 50, 100, and 200 ms SOA conditions, respectively. Each probe display remained on screen for half of the given SOA duration, followed by an equivalent duration "blank" screen containing only the fixation cross. Search displays remained on screen for 100 ms, followed by a 100 ms "blank" screen, regardless of the given SOA duration. Participants were tasked with responding after each search display to indicate whether the target color had appeared in the top or bottom half of either cloud by pressing the up and down keys, respectively.

intervals throughout a series of 12 trials (1600 ms each). The colored dots appeared in four unique equiluminant colors (two colors in each cloud), one of which was always pre-defined as the target color. Every 1600 ms, the colored dots within these clouds would form a search display including four separately colored semicircular areas, and participants were tasked with reporting the vertical location of the target-colored area (Figure 1, top right). During the period between two successive search displays, the clouds formed a sequence of probe displays, wherein the colored dots within each cloud became randomly interspersed so as not to produce any distinguishable shape or pattern (Figure 1, top left).

As before, these target-color probes were employed to track the temporal profile of search template activation processes. Each individual probe display was presented briefly and always included dots that matched the target color as part of one cloud, either on the left or right side. As in our previous work (Dodwell et al., 2024; Grubert & Eimer, 2018, 2019, 2020), template activation states were assessed by measuring N2pc components in response to each of these probe displays. During the time when the target-color template is active, lateral dots that match the color of the target will attract attention, and should thus trigger an N2pc (i.e., an enhanced negativity contralateral to the side where the target-color dots are presented). In contrast, no such contralateral effect will be elicited during time periods where this template is inactive. Importantly, the side on which these target-color dots appeared was randomly and independently determined for each successive probe display, ensuring that there were no sequential dependencies of target-color dot locations between individual probe displays. Analogously, the location of the target-color area in the search displays was not correlated

14698986, 2024, 8, Downloaded from https://onlinelibrary.wiley.com/doi/10.1111/psyp.14582 by Test, Wiley Online Library on [08/07/2024]. See the Terms and Conditions (https://onlinelibrary.wiley.com/terms-and-conditions) on Wiley Online Library for rules of use; OA articles are governed by the applicable Creative Commons License

with the location of any preceding target-color probes. This ensured that lateralized N2pc components for each successive target-color probe, and the search target could be computed separately and independently despite these stimuli being presented in rapid succession.

It should be noted that these probe presentation procedures somewhat resemble those commonly employed in EEG studies that measure steady-state visual evoked potentials (SSVEPs) to assess different aspects of attentional selectivity (see Andersen et al., 2011, for review). More specifically, several of these studies have employed superimposed random-dot kinematograms (RDKs) in two different colors to track facilitatory and inhibitory aspects of feature-based attention (e.g., Andersen & Müller, 2010; Störmer & Alvarez, 2014). In these studies, dots of target and distractor colors flickered at different frequencies to trigger distinct SSVEPs, allowing SSVEP amplitude differences observed at the target versus distractor frequencies to be employed as markers of feature-selective effects on the visual processing of task-relevant displays. Despite the similarities in the stimuli used, the goals and methods employed in the present study were substantially different. We focused on preparatory processes activated prior to the arrival of task-relevant visual input and on feature-selective modulations of visual activity in the time domain (N2pc components) rather than in the frequency domain (SSVEPs).[1]

In an attempt to maximize temporal sampling, new probe displays were presented every 50 ms, which should in principle allow search template activation to be independently probed at a frequency of 20 Hz (i.e., 28 times in total during the period between two search displays). If target-color templates are indeed activated anew on each trial (as suggested by our previous observations, e.g., Grubert & Eimer, 2018), probe N2pcs should be absent for early probes and emerge at a specific point during the preparation period. Furthermore, if search templates are sensitive to expectations with respect to the arrival time of the next search display, these probe N2pcs should increase in amplitude toward the end of this period. This dense temporal sampling of probe-triggered N2pcs also allows for improving the signal-to-noise ratio of individual N2pc components, specifically by averaging the N2pc waveform of probe N with that of probes $N-1$ and $N+1$. Applying such a smoothing procedure might help to obtain an even clearer picture of the emergence and time course of probe N2pcs. It was applied to the data of each sequential probe except those occurring directly before or after a search display (e.g., probes 2–27).

While the RSPP–HD procedure should theoretically reveal the existence and precise time course of preparatory search template activation, in practice, sampling these processes at a rate of 20 Hz might exceed the temporal limitations for triggering independent template-guided attention shifts and/or N2pc components in rapid succession. We therefore also included a second condition where sampling rate was halved, and new probe displays only appeared every 100 ms. Furthermore, we also included a third condition where sampling frequency was again halved, with an interval of 200 ms between the onset of successive probe displays, which matches the temporal parameters employed as in our earlier studies with color singleton probes.

2 | METHODS

2.1 | Participants

A total of 18 participants took part in the study ($M=27.9$ years, $SD=7.5$ years, fourteen female, three left-handed). All participants provided written consent prior to testing, reported normal or corrected-to-normal vision, and were monetarily compensated upon completion of the study. The sample size of 18 exceeded the minimum of 16 datasets necessary to achieve sufficient statistical power, as estimated by an apriori power analysis ($\alpha=0.05$, $1-\beta=.80$, $f=1.46$; G*Power; Faul et al., 2007). The effect size used in this analysis was based on the amplitude of N2pc components triggered by color-singleton probe stimuli, which were observed in previous research using the relatively similar RSPP procedure (see the main effect of laterality for target-colored probes in the "Search Task"; Dodwell et al., 2024). The present study was conducted in accordance with the Declaration of Helsinki and approved by the Psychology Ethics Committee at Birkbeck, University of London.

2.2 | Materials

The experiment was presented on a 24.5-in monitor (BenQ Zowie XL2546; TN panel, 1920 × 1080 resolution, 240 Hz refresh rate) at a viewing distance of approximately 100 cm, controlled by a Windows 10 PC (Acer PO3-630; Intel Core i7-11700F, NVIDIA GeForce RTX 3070). The luminance of all stimuli was determined directly on the experimental monitor against the same dark gray background that was used during stimulus presentation, using a high-precision luminance meter (Konica Minolta LS-100). The experimental script was coded in Python (ver. 3.9.13) using the Psychopy toolbox (ver. 2022.2.3; Peirce et al., 2019). Participants completed the experiment while seated in an electromagnetically shielded, sound-damped, temperature controlled, and dimly lit cabin.

[1]Because target-color and nontarget-color dots always flickered at the same frequency in different task conditions (20, 10, or 5 Hz), it was also not possible to isolate color-selective effects through frequency tagging.

14698986, 2024, 8, Downloaded from https://onlinelibrary.wiley.com/doi/10.1111/psyp.14582 by Test, Wiley Online Library on [08/07/2024]. See the Terms and Conditions (https://onlinelibrary.wiley.com/terms-and-conditions) on Wiley Online Library for rules of use; OA articles are governed by the applicable Creative Commons License

To record the EEG data, 61 of 64 active Ag/AgCl electrodes connected to a digital amplifier (ActiCAP slim/snap & BrainAmp DC; Brain Products GmbH, Gilching, Germany) were placed over scalp positions according to the international 10–10 system (electrode sites: Fp: z, 1, 2 | AF: 3, 4, 7, 8 | F: z, 1, 2, 3, 4, 5, 6, 7, 8, 9, 10 | FC: 1, 2, 3, 4, 5, 6 | FT: 7, 8 | T: 7, 8 | C: z, 1, 2, 3, 4, 5, 6 | CP: z, 1, 2, 3, 4, 5, 6 | TP: 7, 8 | P: z, 1, 2, 3, 4, 5, 6, 7, 8 | PO: z, 3, 4, 7, 8 | O: z, 1, 2 | VEOG, HEOG-L, HEOG-R). The three remaining electrodes were placed over the inferior orbit of the left eye and the outer canthi of each eye to monitor vertical and horizontal eye movements. Impedances were kept below 10 kΩ, with the electrodes located over AFz and FCz serving as an online ground and reference. The raw EEG signals were continuously sampled at 1 kHz while being digitally low- and high-pass filtered (250 Hz and 0.01 Hz) as they were recorded, using a dedicated Windows 10 PC (Dell Precision 5820, Intel Xeon W-2235, NVIDIA Quadro P2200) running BrainVision Recorder (ver. 1.25.0001, Brain Products GmbH, Gilching, Germany). The delay in event timings between the presentation and recording computers was verified to be no greater than 1 ms.

2.3 | Experimental design

The HD-RSPP paradigm employed in the present study comprised a series of task-irrelevant probe displays presented at regular intervals between successive task-relevant search displays (see Figure 1, bottom for a depiction of the trial sequence). The probe and search displays were composed of two ring-shaped clouds of colored dots presented on a dark gray background (CIE $x/y = 0.285/0.347$; 5.25 cd/m^2), appearing 6.5° of visual angle to the left and right of a gray central fixation cross (0.4 × 0.4° visual angle; 0.291/0.333; 24.0 ± 0.3 cd/m^2). Each cloud included 171 individual dots (0.25° visual angle ø) anchored to evenly spaced points along the radii of six concentric rings (2.88°, 4.04°, 5.20°, 6.35°, 7.51°, and 8.66° visual angle ø, respectively). Initially, each dot was randomly positioned along a radius (0.29° visual angle ø) surrounding its respective anchor point. Then, in each subsequent display, a new position would be randomly selected from a 120° arc directly opposing the previous. As such, the dots in each cloud could not spatially overlap within a given display nor coherently shift between consecutive displays.

Within each cloud, the dots appeared in equal proportions of two unique colors, for a total of four equiluminant colors present in each display (orange: 0.504/0.440, green: 0.296/0.579, blue: 0.181/0.189, purple: 0.207/0.095; all 24.0 ± 0.3 cd/m^2). As such, each color could only appear on one side of the screen at any time, providing the lateralization necessary for a pre-defined target color to elicit an N2pc component. The lateral locations of both the target and non-target colors were pseudo-randomized per display, such that their lateral positions and pairings remained unpredictable but nevertheless counterbalanced across the entire experiment. In probe displays, the colors of the dots within each cloud were pseudo-randomly assigned so as not to produce any discernible pattern or structure (Figure 1, top left). Conversely, in search displays, the dots appearing in the top and bottom half of each cloud were assigned uniformly separate colors, thus producing a discernibly "split" structure (Figure 1, top right). Participants were tasked with indicating whether the target color appeared in the top or bottom half of its respective cloud (irrespective of lateral position) by pressing the "up" or "down" arrow keys accordingly.

The experiment was segmented into three runs of 24 blocks each, with 12 trials per block. Trials ran consecutively – that is, without pause between the end of one and the start of the next. As such, participants entered their responses to the search display of the preceding trial during the probe display series of the following trial. To examine the temporal resolution with which template activity could be reliably traced, three probe SOA conditions of 50, 100, and 200 ms were tested. Each probe display within a given condition remained on screen for exactly half of the respective SOA duration, followed by an equivalent duration "blank" screen containing only the fixation cross prior to the onset of the next display. In all three conditions, search displays were presented for 100 ms, followed by a 100 ms blank screen before the probe series of the next trial would begin. Each trial (including the series of probe displays and the search display) lasted for a total of 1600 ms, resulting in 28, 14, and 7 probe displays per trial in the 50, 100, and 200 ms conditions, respectively. Each block was pseudo-randomly assigned a condition and target color, ensuring there were 24 blocks of each condition and that the four stimuli colors would define the target in 18 blocks each. Live visualizations of the stimulation sequence in all three conditions can be observed at the following URL: https://gordondodwell.github.io/RSPP_HD/.

2.4 | EEG processing

The EEG data were processed using MNE Python (ver. 1.3.0, Gramfort et al., 2013). The continuous data of each participant (including all three runs of 24 blocks) were first passed through a 0.1 Hz high-pass FIR filter to remove low-frequency noise, as well as an FIR notch filter in 50 Hz intervals between 50 and 250 Hz to remove line noise. The continuous data were then manually inspected to identify

14698986, 2024, 8, Downloaded from https://onlinelibrary.wiley.com/doi/10.1111/psyp.14582 by Test, Wiley Online Library on [08/07/2024]. See the Terms and Conditions (https://onlinelibrary.wiley.com/terms-and-conditions) on Wiley Online Library for rules of use; OA articles are governed by the applicable Creative Commons License

and remove bad channels, segments where substantial artefacts could be identified, or blocks where the participants' error rate exceeded 35% (where it was considered likely the participant had responded to the incorrect target color). An extended Picard independent component analysis (ICA) was then performed across all 64 channels of the continuous data (61 EEG, 3 EOG, 500 steps, convergence bound = 1×10^{-7}), to identify and remove components representing EOG artifacts prior to a back projection of the residuals. A 40 Hz low-pass FIR filter was then applied to remove high-frequency noise, after which all EEG signals were re-referenced to the 61-channel common average. The data was then segmented relative to the onset of the target and probe displays within each SOA condition (50: probes 1–28; 100: probes 1–14; 200: probes 1–7), with epochs including a 100 ms prestimulus baseline and the 400 ms thereafter. An automatic, amplitude-driven artifact rejection was then performed on the epoched data based on a generalized ESD test (alpha-threshold 0.05) implemented in the OHBA Software Library (OSL; https://ohba-analysis.github.io/). This resulted in an average of 1.3% ($M = 198$, $SD = 152$) of epochs being rejected across all participants. Per condition, ERP waveforms contralateral and ipsilateral to the location of the target color in each probe and search display were then calculated at the lateral posterior electrodes PO7 and PO8, along with the respective N2pc component waveforms (the contralateral – ipsilateral difference wave).

2.5 | Statistical analysis

2.5.1 | Behavioral analysis

For each participant, error rates (ERs) were first calculated per block, with blocks exceeding 35% errors being removed from further analysis and the ERs of the remaining blocks being averaged per condition. Mean response times (RTs) were then calculated per condition, excluding erroneous responses as well as those faster than 200 ms or slower than 1500 ms (e.g., anticipations and responses occurring during the subsequent search display). The per-condition RTs and ERs of each participant were then analyzed within two separate one-way repeated measures ANOVAs, to test for potentially differential effects between each of the SOA conditions (50, 100, and 200 ms).

2.5.2 | ERP analysis

To determine an appropriate time window for analysis, the N2pc waveforms relative to both the target display and any probe displays occurring within 200 ms prior were grand averaged across participants for each condition, as lateralization was most consistently apparent in this timeframe (50 ms: probes 25–28 | 100 ms: probes 13 & 14 | 200 ms: probe 7). The mean of the 50% onset and offset times of the most negative peaks detected in these grand-averaged waveforms was then calculated, resulting in an 80 ms time window beginning 190 ms after stimulus onset. Within this window, the mean amplitudes of the contralateral and ipsilateral ERPs and their relative N2pc waveforms were then calculated per participant for the probe and target displays of each condition.

For each condition, analysis of the ERP responses to probe displays focused on determining at which latencies N2pcs were elicited and whether N2pc amplitudes increased toward the end of the preparation period. The ERP mean amplitudes of each probe display were first submitted to a $2 \times N$ repeated-measures ANOVA, with factors of Laterality (contralateral vs ipsilateral to the target color) and Probe Latency (probes $1-N$; N being the condition-relative number of probes). Pairwise Bayesian comparisons were also conducted between the ERP mean amplitudes at each probe latency, validating the presence or absence of the N2pc component on a per-probe basis. These were followed by cluster-based permutation analyses (Maris & Oostenveld, 2007) performed between the contralateral and ipsilateral waveforms of each probe display, using 25,000 permutations to cluster significantly more negative contralateral timepoints (one-tailed, alpha level of 0.05). This cluster-based permutation approach complements the more traditional statistical analyses detailed above by providing a convergent, non-parametric measure to determine the probability of differences between EEG time series (see Dodwell et al., 2024 for more detail). Lastly, to determine whether N2pc amplitudes increased toward the end of the preparation period, a follow-up $2 \times N$ repeated measures ANOVA (with factors of "Laterality" × "Probe Latency") was conducted, including only those probes which Bayesian comparisons indicated to have elicited a continuous series of N2pcs prior to search display onset.

The amplitudes of the N2pc components elicited by the search displays of each condition were also compared to check for potential effects of the differential presentation times between the search and probe displays. This was done by submitting the contralateral and ipsilateral ERPs from the search displays of all three conditions to a 2×3 repeated-measures ANOVA, with factors of Laterality (contralateral vs ipsilateral to the target color) and Condition (50, 100, and 200 ms).

Addit, we made use of the dense temporal sampling of template activation in the 50 ms SOA condition by averaging the waveforms of each set of three successive probes centered on probe N ($N-1$, N, $N+1$). This "smoothing"

14698986, 2024, 8, Downloaded from https://onlinelibrary.wiley.com/doi/10.1111/psyp.14582 by Test, Wiley Online Library on [08/07/2024]. See the Terms and Conditions (https://onlinelibrary.wiley.com/terms-and-conditions) on Wiley Online Library for rules of use; OA articles are governed by the applicable Creative Commons License

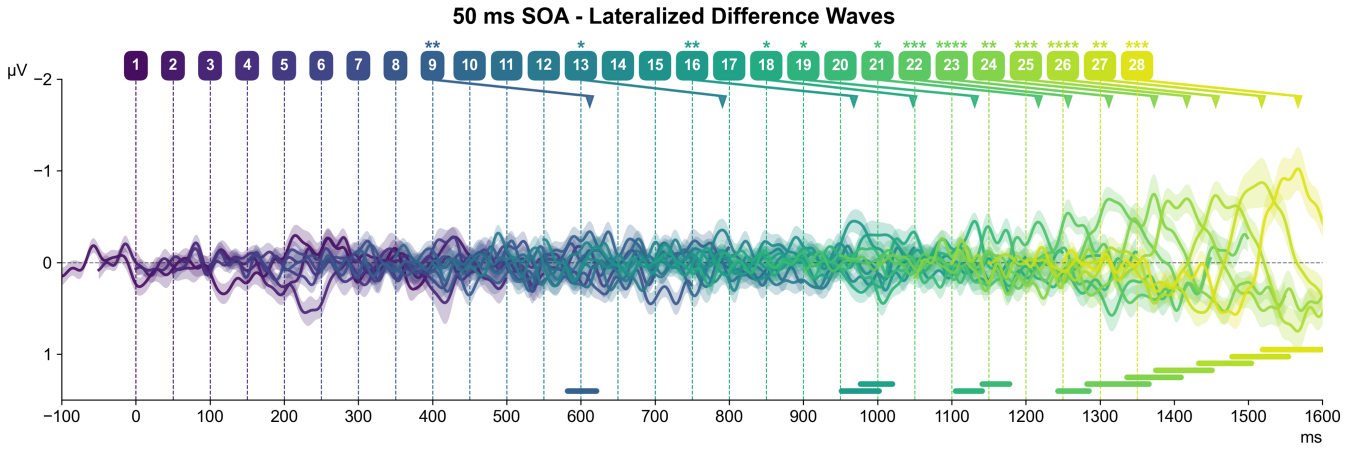

FIGURE 2 Lateralized difference waves (contralateral – ipsilateral waveforms) elicited over scalp sites PO7/PO8 by the series of 28 probe displays in the 50 ms condition. The onset of each probe is indicated by a vertical dotted line in the color of the numbered label above, indicating their serial position across a single trial. The different waveforms of each probe appear in the corresponding label color, beginning 100 ms prior to their relative onset and continuing for 400 ms thereafter. These waveforms overlap within the figure but are spaced in accordance with their temporal occurrence. Waveforms for which Bayesian analyses indicated contralateral negativity within the N2pc time window (190–270 ms after probe onset) are marked above their relative label with asterisks (* = BF_{10} > 3, ** = BF_{10} > 10, *** = BF_{10} > 30, **** = BF_{10} > 100), as well as an arrow over their relative peak. Similarly, portions of waveforms wherein the permutation analysis detected significant clusters of contralateral negativity are marked below with correspondingly colored horizontal bars.

procedure resulted in 26 newly generated waveforms centered on probes 2–27, respectively, where, for example, the "smoothed" waveform for probe 12 was calculated by averaging the "unsmoothed" waveforms of probes 11, 12, and 13. Given the close temporal proximity of successive probes, this approach provided a means to increase the effective signal-to-noise ratio in the 50 ms data threefold without losing the temporal resolution of tracking search template activation, as reflected by the time course of probe N2pcs. Following this smoothing procedure, the entire probe display analysis pipeline was then reapplied to the newly generated "smoothed" data.

3 | RESULTS

3.1 | Behavioral results

The ANOVA of ERs did not reveal an effect of condition (F (2,34) = 0.19, p = .83, η^2G = 0.003), indicating that there were no substantial differences between the mean error rates of each condition (50 ms: M = 3.77%, SD = 2.25% | 100 ms: M = 3.51%, SD = 1.92% | 200 ms: M = 3.58%, SD = 2.35%). By contrast, the ANOVA of RTs did demonstrate a significant main effect of condition (F (2,34) = 29.49, p < .001, η^2G = 0.105), as response times were fastest in the 200 ms condition (M = 400 ms, SD = 50 ms), moderate in the 100 ms condition (M = 420 ms, SD = 49 ms), and slowest in the 50 ms condition (M = 443 ms, SD = 57 ms). Follow-up one-tailed pairwise comparisons confirmed RTs to be significantly slower in the 50 ms condition as compared to both the 100 ms (t(17) = 3.94, p = .001, d = 0.43) and 200 ms conditions (t(17) = 5.90, p < .001, d = 0.79), as well as in the 100 ms condition as compared to the 200 ms condition (t(17) = 7.56, p < .001, d = 0.40).

3.2 | EEG results

3.2.1 | Probe N2pcs in the 50 ms condition

Figure 2 shows the lateralized difference waves of the 28 successive probes in the 50 ms condition. The ERPs from which these difference waves were calculated are included in the supplementary information (Figure S1). N2pcs began to emerge between probes 9 and 13 (1000–800 ms before search display onset) and were consistently elicited from probe 21 onward (400 ms before search display onset). N2pc amplitudes also appeared to steadily increase from probe 21 towards the end of the preparation period.

The ANOVA results indicated a significant main effect of Laterality (F (1,17) = 19.60, p < .001, η_p^2 = 0.54), confirming the presence of N2pcs to target colored probes. A significant Laterality * Probe Latency interaction was also detected (F (27,459) = 5.09, p < .001, η_p^2 = 0.23), confirming that amplitudes within the N2pc time window differed across the 28 consecutive probe displays. Bayesian comparisons demonstrated decisive evidence for the presence of N2pcs at probes 23 (BF_{10} = 279.52, d = 0.83) and 26 (BF_{10} = 361.45, d = 0.98), as well as very strong evidence at probes 22 (BF_{10} = 47.92, d = 0.48), 25 (BF_{10} = 48.62, d = 0.74), and 28 (BF_{10} = 80.00, d = 0.33). There was also

14698986, 2024, 8, Downloaded from https://onlinelibrary.wiley.com/doi/10.1111/psyp.14582 by Test, Wiley Online Library on [08/07/2024]. See the Terms and Conditions (https://onlinelibrary.wiley.com/terms-and-conditions) on Wiley Online Library for rules of use; OA articles are governed by the applicable Creative Commons License

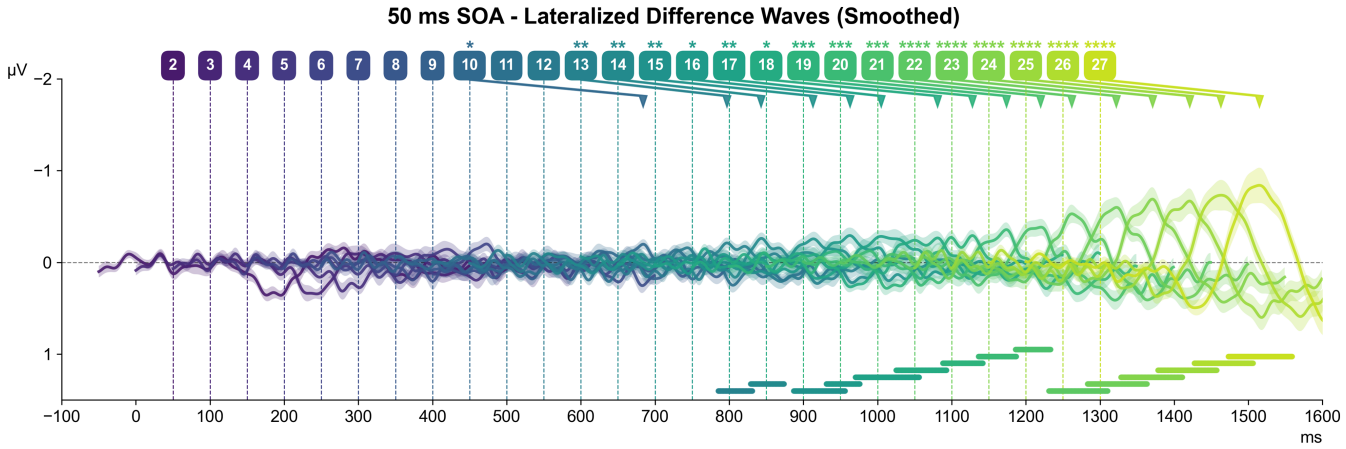

FIGURE 3 Lateralized difference waves elicited by the series of 28 probe displays in the 50 ms condition, with averaging across the three successive waveforms centered on probe N ($N-1$, N, $N+1$) applied to probes 2–27. As this smoothing procedure was not applied to probes 1 and 28, these waveforms are excluded. The structure and layout of Figure 3 are otherwise identical to that of Figure 2.

strong evidence of N2pcs at probes 9, 16, 24, and 27 (all $BF_{10} \geq 15.55$, all $d \geq 0.20$), with moderate evidence at probes 13, 18, 19, and 21 (all $BF_{10} \geq 3.09$, all $d \geq 0.19$). Bayesian analysis did not demonstrate evidence for the presence of N2pcs within the waveforms of the remaining probes (1–8, 10–12, 14–15, 17, 20; all $BF_{10} \leq 2.05$, $d \leq 0.34$). The results of the permutation analysis generally complimented those of the Bayesian comparisons, suggesting the presence of N2pcs for probes 9, 16, 17, 19, 20, and continuously from probes 22 to 28. To assess whether N2pc amplitudes increased toward the end of the preparation period, a follow-up ANOVA was performed across probes 21–28, as this series of probes was shown by the Bayesian comparisons to continuously elicit N2pcs up until the onset of the search display. This ANOVA revealed a significant Laterality * Probe Latency interaction (F (7,119) = 2.58, $p = .016$, $\eta_p^2 = 0.13$), confirming that the amplitude of the N2pc's gradually increased toward the end of the preparation period.

3.2.2 | 50 ms condition: Smoothed averages

Figure 3 provides the lateralized difference waves from the 50 ms condition, following the application of averaging across three successive probes ($N-1$, N, $N+1$) to the waveforms of probes 2–27 (see Figure S2 in the supplementary information for the contralateral and ipsilateral ERPs on which these difference waves were based). As this smoothing procedure could not be applied to probes 1 and 28, their data were excluded from both the figure and statistical analysis. The smoothing procedure successfully reduced apparent noise in the data, providing a substantially clearer emergence and build-up of N2pcs toward the end of the preparation period. N2pcs began to emerge as early as probe 10 (950 ms before search display onset) and were consistently elicited with seemingly steadily growing amplitudes from probe 13 onward (beginning 800 ms prior to the search display).

An ANOVA performed across probes 2–27 demonstrated a significant main effect of Laterality (F (1,17) = 18.66, $p < .001$, $\eta_p^2 = 0.52$), indicating the presence of N2pcs. There was also a significant Laterality * Probe Latency interaction (F (25,425) = 12.16, $p < .001$, $\eta_p^2 = 0.42$), confirming that amplitudes within the N2pc time window differed across the 26 tested probes. Bayesian comparisons indicated decisive evidence for the presence of an N2pc at probes 21–27 (all $BF_{10} \geq 245.06$, all $d \geq 0.46$), as well as very strong evidence at probes 19–21 (all $BF_{10} \geq 38.16$, all $d \geq 0.38$). There was also strong evidence indicated at probes 13, 14, 15, and 17 (all $BF_{10} \geq 18.78$, all $d \geq 0.17$), and moderate evidence at probes 10, 16, and 18 (all $BF_{10} \geq 6.73$, all $d \geq 0.13$). For the remaining probes, substantial N2pc activity was not detected (2–9, 11, 12; all $BF_{10} \leq 2.19$, $d \leq 0.09$). The results of the permutation analysis were closely similar, indicating that N2pcs were consistently elicited from probe 17 onward. A follow-up ANOVA of probes 13–27 demonstrated a significant Laterality * Probe Latency interaction (F (14,238) = 12.29, $p < .001$, $\eta_p^2 = 0.42$), confirming that N2pc amplitudes increased toward the end of the preparation period. This interaction effect persisted even when testing within smaller groups of probes approaching search display onset, e.g., probes 21–24 (F (3,51) = 6.95, $p = .001$, $\eta_p^2 = 0.29$) and 24–27 (F (3,51) = 3.56, $p = .02$, $\eta_p^2 = 0.17$).[2] A gradual increase of the N2pc amplitudes could, therefore, be detected at various points throughout the preparation period – even within 200 ms timespans, which would have constituted a single probe event in the 200 ms condition.

[2]In corresponding analyses based on the original unsmoothed data set, these two interactions were not significant, indicating that the smoothing procedure did indeed improve data quality.

14698986, 2024, 8, Downloaded from https://onlinelibrary.wiley.com/doi/10.1111/psyp.14582 by Test, Wiley Online Library on [08/07/2024]. See the Terms and Conditions (https://onlinelibrary.wiley.com/terms-and-conditions) on Wiley Online Library for rules of use; OA articles are governed by the applicable Creative Commons License

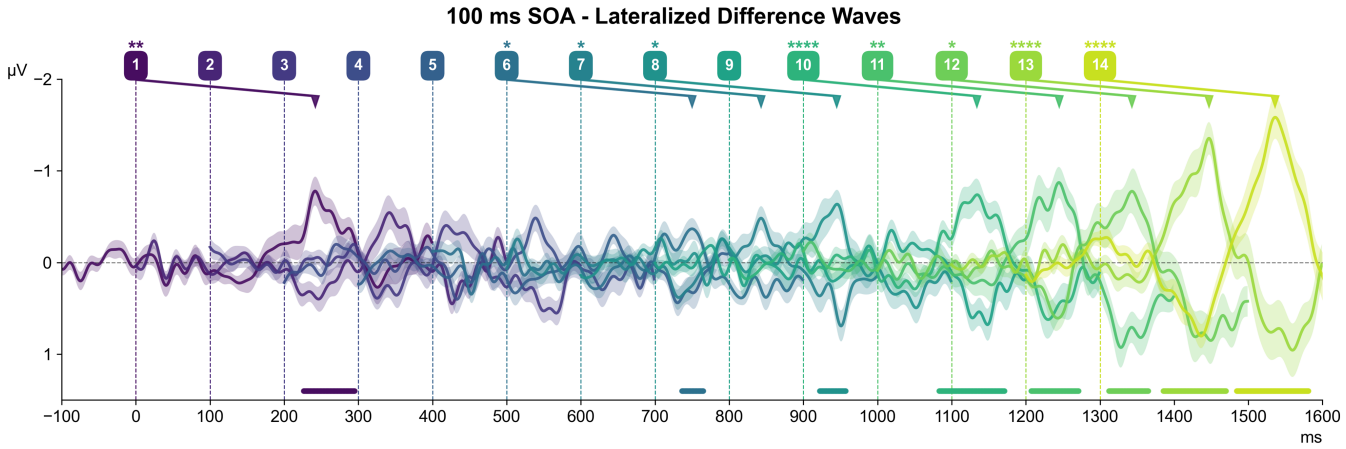

FIGURE 4 Lateralized difference waves elicited by the series of 14 probe displays in the 100 ms condition. The structure and layout of Figure 4 are otherwise identical to that of Figure 2.

3.2.3 | Probe N2pcs in the 100 ms condition

Figure 4 shows the lateralized difference waves elicited by the 14 successive probes in the 100 ms condition (the respective ERPs are provided in the supplementary information; see Figure S3). N2pcs seemingly emerged between probes 6 and 8 (900–700 ms prior to search display onset) and were reliably present from probe 10 onwards (500 ms prior to search display onset). Notably, a substantial N2pc was also elicited by probe 1. Like the activity profile observed in the 50 ms condition, the amplitudes of these N2pcs again appeared to gradually increase from probe 10 onward until the end of the preparation period.

An ANOVA revealed a significant main effect of Laterality (F (1,17) = 12.07, p = .003, η_p^2 = 0.42), coupled with a significant Laterality * Probe Latency interaction (F (13,221) = 9.23, p < .001, η_p^2 = 0.35), confirming that N2pcs of were differentially present within the 14 consecutive probe displays. These effects were confirmed via follow-up Bayesian comparisons between the contra- and ipsilateral waveforms of each probe. There was decisive evidence for the presence of N2pcs at probes 10 (BF_{10} = 171.47, d = 1.03), 13 (BF_{10} = 571.13, d = 1.20), and 14 (BF_{10} = 717.07, d = 0.93), as well as strong evidence at probes 1 (BF_{10} = 14.05, d = 0.22) and 11 (BF_{10} = 19.62, d = 0.94). There was also moderate evidence of N2pcs at probes 6, 7, 8, and 12 (all $BF_{10} \geq 3.89$, all $d \geq 0.19$). Evidence for the presence of N2pcs at the remaining probes (2–5, 9) was inconclusive (all $BF_{10} \leq 2.03$, $d \leq 0.31$). Permutation analysis further supported the observed pattern, indicating the likely presence of N2pcs for probes 1 and 8, then continuously from probes 10 to 14. The follow-up ANOVA across probes 10–14 also indicated a significant Laterality * Probe Latency interaction (F (4,68) = 5.87, p < .001, η_p^2 = 0.26), confirming that the amplitude of the N2pcs present within these probes increased toward the end of the preparation period.

3.2.4 | Probe N2pcs in the 200 ms condition

Figure 5 depicts the lateralized difference waves elicited by the 7 successive probes in the 200 ms condition (see Figure S4 in the supplementary information for the relative ERPs). N2pcs only appeared to emerge at probe 6 (600 ms prior to search display onset), followed by a seemingly more prominent N2pc at probe 7 (400 ms before search onset). There also appeared to be a somewhat less reliable N2pc following probe 1. Nevertheless, N2pc amplitudes still exhibited gradually increasing negativity approaching the end of the preparation period.

In contrast to the conditions detailed prior, the results obtained from the ANOVA did not demonstrate a significant main effect of Laterality (F (1,17) = 3.05, p = .10, η_p^2 = 0.15). However, a significant main effect of Probe Latency (F (6,102) = 8.43, p < .001, η_p^2 = 0.33) and a Laterality * Probe Latency interaction (F (6,102) = 14.69, p < .001, η_p^2 = 0.46) were indicated, confirming the presence of N2pcs as a function of probe latency. Follow-up Bayesian comparisons between the contra- and ipsilateral waveforms of each probe indicated very strong evidence for the presence of an N2pc at probe 7 (BF_{10} = 49.35, d = 0.66), along with moderate evidence at probe 6 (BF_{10} = 6.77, d = 0.41). For all probes prior to probe 6, the Bayesian analysis did not find conclusive evidence for the presence of any N2pcs (all $BF_{10} \leq 1.96$, $d \leq 0.41$). The permutation analysis also indicated the likely presence of an N2pc at probes 6 and 7, although there was also some indication of N2pc activity at probe 1. Finally, a follow-up ANOVA across probes 6 and 7 also revealed the presence

14698986, 2024, 8, Downloaded from https://onlinelibrary.wiley.com/doi/10.1111/psyp.14582 by Test, Wiley Online Library on [08/07/2024]. See the Terms and Conditions (https://onlinelibrary.wiley.com/terms-and-conditions) on Wiley Online Library for rules of use; OA articles are governed by the applicable Creative Commons License

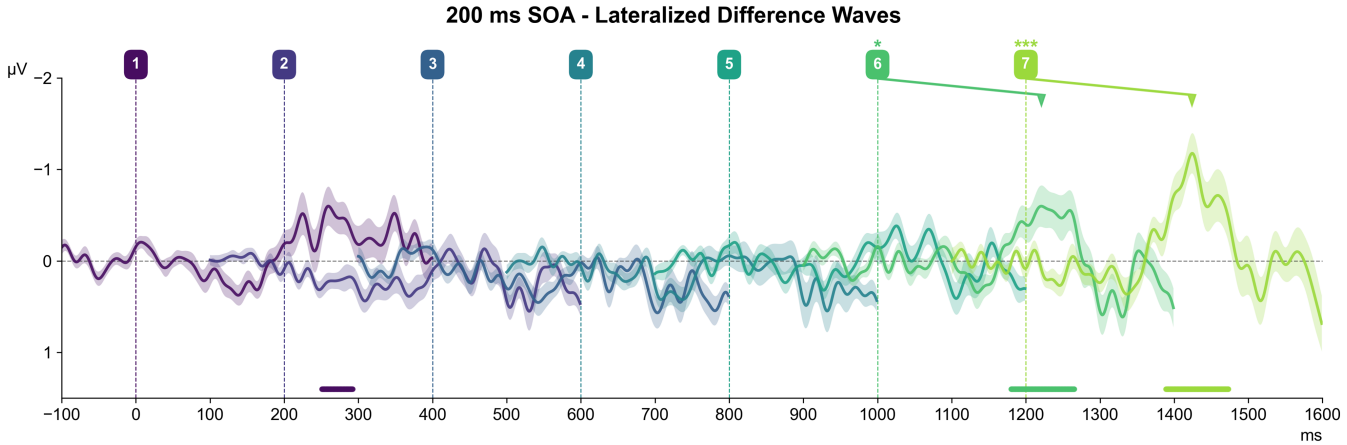

FIGURE 5 Lateralized difference waves elicited by the series of 7 probe displays in the 200 ms condition. The structure and layout of Figure 5 are otherwise identical to that of Figures 2 and 4.

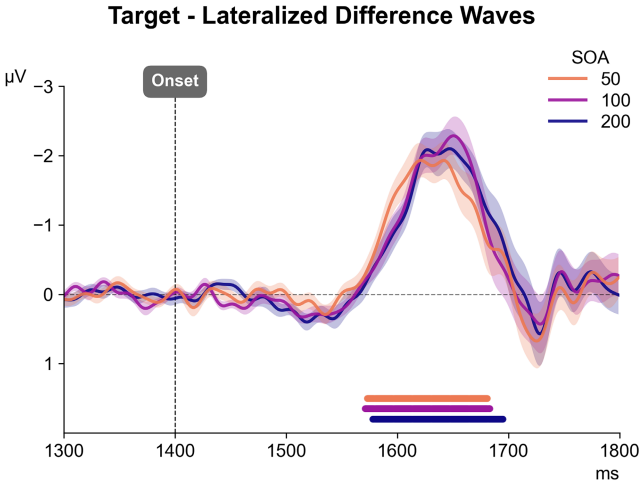

FIGURE 6 Target N2pc difference waves (contralateral – ipsilateral waveforms) elicited over scalp sites PO7/PO8 by the search displays of each condition (50 ms: orange | 100 ms: red | 200 ms: purple). The time series of each waveform begins 100 ms prior to the search display onset (indicated by the vertical dotted line) and ends 400 ms thereafter. Portions of waveforms wherein permutation analyses indicated significant clusters of contralateral negativity are marked below with correspondingly colored horizontal bars.

of a significant Laterality * Probe Latency interaction (F (1,17) = 5.65, p = .029, η_p^2 = 0.25).

3.2.5 | Between-condition target N2pc comparisons

Figure 6 presents the overlayed target N2pc difference waves elicited by the search displays for each SOA condition, along with the results of cluster-based permutation testing between the per-condition contra- and ipsilateral waveforms. An ANOVA revealed a significant main effect of Laterality (F (1,17) = 61.94, p < .001, η_p^2 = 0.79), confirming the presence of N2pcs, along with a significant main effect of Condition (F (2,34) = 12.26, p < .001, η_p^2 = 0.42), suggesting that the contralateral and ipsilateral waveforms differed overall between the 50, 100, and 200 ms conditions. However, no significant interaction was detected, indicating that the amplitude of the N2pc waveforms was not substantially dissimilar between conditions.

4 | DISCUSSION

Representations of target-defining features (attentional templates) play a crucial role in the guidance of attentional selectivity during visual search (e.g., Desimone & Duncan, 1995; Eimer, 2014). To be maximally effective in rapidly guiding attention toward target objects among multiple distractors in search displays, these templates should already be activated during the preparation for search, prior to any neural or behavioral responses to these displays being triggered. Because of the covert nature of preparatory template activation processes, it has been challenging to obtain any direct evidence for their presence, their time course, or their sensitivity to task-induced expectations and intentions.

Here, we present a novel approach to track these processes in real time with neural measures. Our high-definition RSPP paradigm was specifically designed to overcome the problems of previous attempts to measure search template activation, where probes were salient singletons (potentially triggering exogenous attentional capture) that were presented relatively infrequently and always at task-irrelevant locations.

In the current study, both the probe and search displays were homologously formed by "clouds" of rapidly changing colored dots. The display types only differed in

14698986, 2024, 8, Downloaded from https://onlinelibrary.wiley.com/doi/10.1111/psyp.14582 by Test, Wiley Online Library on [08/07/2024]. See the Terms and Conditions (https://onlinelibrary.wiley.com/terms-and-conditions) on Wiley Online Library for rules of use; OA articles are governed by the applicable Creative Commons License

the distribution of colors across each cloud, being randomly interspersed in the probe displays while forming organized, semi-circular quadrants in the search displays. Critically, in all displays, one cloud always randomly included the pre-defined target color, thereby serving as either a probe or target. Although the probe displays were entirely task-irrelevant, they were still predicted to attract attention if presented during periods when the corresponding target-color search template was active, which would be reflected by the presence of reliable N2pc components to those probes.

Results demonstrated that this new cloud probe procedure was indeed successful in tracking the activation of target-color search templates during the period between two search displays, and that it was able to do so with high temporal resolution. When the cloud probe displays changed every 50 ms, specific target-color probes elicited clear N2pc components, and the temporal pattern of probe N2pcs showed a distinctive time course during the preparation period between two search displays. Reliable probe N2pcs were consistently present from 400 ms prior to the onset of the next search display and increased in size toward the end of the preparation period. These observations demonstrate that target-color probes attracted attention well before the next search display was presented and imply that a corresponding search template was triggered in a proactive fashion during this period. In contrast, there was little evidence for the presence of reliable probe N2pcs during the first 800 ms after the offset of the previous search display, which suggests that no target-color template was active during the first half of the preparation period. This absence of early target-color probe N2pcs might be due to interference resulting from processing the preceding target and selecting a corresponding response during this period. However, we have previously found analogous results even when no target was present in the preceding trial (Grubert & Eimer, 2018; Exp.2), suggesting that this temporal pattern of probe N2pcs is not exclusively driven by competitive interactions between search templates and target processing.

By smoothing the data from the 50 ms SOA condition across probes $N-1$, N, and $N+1$, the presence and temporal pattern of probe N2pcs became even clearer (see Figure 3), demonstrating that this smoothing procedure was successful in improving data quality and refining the gradual increase of probe N2pc amplitudes toward the point in time when the next search display was expected. With this procedure, reliable probe N2pc components now also emerged earlier than in the original analysis across individual probe N2pc data. They were observed consistently for all successive probes from probe 13 onward (i.e., from about 800 ms prior to the onset of the next search display). This indicates that increasing signal strength with this smoothing procedure makes it possible to detect the earliest stages of search template activation. Importantly, even when signal quality was increased in this way, there was no evidence for the presence of probe N2pcs during the first few hundred milliseconds of each trial, providing additional evidence that the search template was not active during this period.

These observations were fully confirmed when the frequency of template activation sampling was halved, with new probes only appearing every 100 ms. In this condition, clear probe N2pcs appeared consistently for the final four probes prior to search display onset (i.e., during the final 500 ms of the preparation period) but were absent or much smaller and less reliable for earlier probes. N2pc amplitudes were again the largest for probes that appeared immediately prior to search display onset. When the temporal sampling frequency was reduced further still, with new probes only appearing every 200 ms (analogous to the procedures used in our previous studies with color singleton probes; e.g., Grubert & Eimer, 2018), only the final two probes during the preparation period triggered reliable N2pcs. Thus, the temporal profile of probe N2pc components in all three unsmoothed temporal sampling conditions reflects the same underlying dynamics of target color templates being activated about 400–500 ms prior to the anticipated arrival of the next search display. Importantly, increasing the sampling frequency by reducing the interval between successive probes did not affect the quality of probe-induced N2pc components, which demonstrates the power of the new RSPP–HD procedure to track the temporal profile of covert search template activation with high precision.

Our results confirm previous suggestions that even in tasks where a target-defining color remains constant across trials and blocks, corresponding target-color templates are not kept activated in a sustained fashion but are instead switched off at the end of one search episode and then switched on again during preparation for the next. They also show that probe N2pcs increased in amplitude toward the end of the preparation period, demonstrating that temporal expectations about the onset of the next search display strongly affect the time course of preparatory target template activation. This probe N2pc amplitude increase can be interpreted in two different ways. On the one hand, it could suggest that the search template activation increased gradually on each trial toward the end of the preparation period. Alternatively, it is possible that search templates only have two activation states (on or off), and that larger N2pc amplitudes for later probes reflect the temporal variability in the onset of template activation processes across trials. Because in each trial the probability that a target-color template is switched

14698986, 2024, 8, Downloaded from https://onlinelibrary.wiley.com/doi/10.1111/psyp.14582 by Test, Wiley Online Library on [08/07/2024]. See the Terms and Conditions (https://onlinelibrary.wiley.com/terms-and-conditions) on Wiley Online Library for rules of use; OA articles are governed by the applicable Creative Commons License

on increases toward the end of the preparation period, later probes would on average accumulate larger N2pcs than earlier probes simply because they attract attention on a larger proportion of trials. As N2pc components can only be derived from averaging EEG activity across multiple trials, it is difficult to distinguish between these two possibilities.

As noted earlier, the quality of probe N2pc components and their temporal profile was very similar regardless of whether the interval between the onset of successive probes was 50, 100, or 200 ms. This shows that even the fastest temporal sampling frequency used here did not exceed the time constraints for triggering multiple independent template-guided shifts of spatial attention by template-matching objects that appear in rapid succession, and thus for tracing the time course of template activation with high-temporal precision. It is important to emphasize that this was achieved despite the fact that probe displays were presented in rapid succession, thus triggering ERP responses that inevitably overlapped in time (as is evident in the contralateral and ipsilateral ERP waveforms included in the supplementary information). This temporal overlap of non-lateralized ERPs does not compromise the extraction of lateralized responses to the target-color dots for individual bilateral cloud displays because the side where these dots appeared was selected independently for each display (i.e., each probe display was equally likely preceded and followed by a display where target-color dots were presented on the same or the opposite side). As a result, subtracting ipsilateral from contralateral ERPs for any particular probe display will reveal lateralized activity for that display only, without any overlap of lateralized responses to the preceding or following probe (or search) display.

Evidence for very fast successive attentional allocation processes has previously been observed for separate target objects that appear in rapid succession at different locations (e.g., Eimer & Grubert, 2014). The presence of such fast parallel template-guided biases in visual processing is in line with a fundamental assumption of the biased competition account of visual attention (e.g., Desimone & Duncan, 1995; Duncan, 2006). According to this account, currently active task sets can bias visual processing in favor of set-matching visual objects at multiple locations, thereby increasing the probability that one or more of these objects will win the competition for attentional selection. The current observations suggest that such parallel attentional biases are not just triggered in response to currently task-relevant visual input, but are already present once observers activate feature-specific target templates for the guidance of attention in an upcoming selection task. In this context, it is notable that clear N2pc components indicative of template-guided attentional capture were triggered by target-color dot clouds in the 50 ms SOA condition despite their presence and location in individual displays being subjectively very hard to detect (as illustrated in the visualizations; https://gordondodwell.github.io/RSPP_HD/). Whether observers remain able to report the side of target-color items in this condition with above-chance accuracy will need to be addressed with forced-choice discrimination procedures. Regardless of the outcome of these future experiments, the current results demonstrate the ability of attentional biases triggered by currently active search templates to selectively affect responses to near-threshold visual stimulation.

Overall, the current results acquired with the new RSPP–HD method confirmed previous observations obtained with the singleton probe procedure (e.g., Grubert & Eimer, 2018), albeit with much improved temporal resolution. This suggests that, at least in the current context of visual search for color-defined target objects, this singleton-based procedure can also be used to obtain insights into the nature of color-specific search template activation processes. However, the new procedures introduced here do have clear advantages. In addition to tracking covert attentional preparation processes with higher temporal resolution, they can measure these preparation processes for the locations that are relevant for an upcoming attentional selection task, and without running any risk of confounding template-guided and salience-driven attention shifts. Moreover, as demonstrated in this study, applying a smoothing procedure to such densely sampled data by averaging across three successive probes can considerably improve its signal-to-noise ratio, thereby increasing the probability of detecting even small or temporally more variable template activation processes.

The possibility of directly observing task-selective top-down attentional preparation mechanisms with objective neural markers unveils numerous new opportunities for investigating the nature and temporal dynamics of attentional task settings in many different contexts. With respect to preparatory attentional templates in visual search, there are many unresolved questions that could be put to the test with this methodology. For example, the nature of search templates that are used in tasks where targets are defined by a conjunction of features from different dimensions has yet to be specified. Other questions include the dynamics of switching between target templates in tasks where search targets change in a predictable fashion, the impact of temporal and feature-based predictions on template activation, or the roles of task difficulty and a priori target probabilities. All these factors may have a distinctive impact on preparatory target preparation processes which may be revealed via tracking these processes in real time.

14698986, 2024, 8, Downloaded from https://onlinelibrary.wiley.com/doi/10.1111/psyp.14582 by Test, Wiley Online Library on [08/07/2024]. See the Terms and Conditions (https://onlinelibrary.wiley.com/terms-and-conditions) on Wiley Online Library for rules of use; OA articles are governed by the applicable Creative Commons License

AUTHOR CONTRIBUTIONS

Gordon Dodwell: Conceptualization; data curation; formal analysis; investigation; methodology; project administration; software; validation; visualization; writing – original draft; writing – review and editing. **Rebecca Nako:** Conceptualization; funding acquisition; investigation; methodology; project administration; resources. **Martin Eimer:** Conceptualization; formal analysis; funding acquisition; methodology; project administration; resources; supervision; writing – original draft; writing – review and editing.

FUNDING INFORMATION

This study was supported by the Economic and Social Research Council (ESRC; grant reference ES/V002708/1).

CONFLICT OF INTEREST STATEMENT

The authors report no conflicts of interest.

DATA AVAILABILITY STATEMENT

The raw, per-participant EEG and behavioral data, as well as the associated analysis scripts, have been anonymized and made available in an OSF repository at the following doi: 10.17605/OSF.IO/DR5WY. To request the Python script of the experimental procedure, please contact the authors directly.

ORCID

Gordon Dodwell https://orcid.org/0000-0001-6772-9849
Rebecca Nako https://orcid.org/0000-0003-1073-414X
Martin Eimer https://orcid.org/0000-0002-4338-1056

REFERENCES

Andersen, S. K., & Müller, M. M. (2010). Behavioral performance follows the time course of neural facilitation and suppression during cued shifts of feature-selective attention. *Proceedings of the National Academy of Sciences*, *107*(31), 13878–13882. https://doi.org/10.1073/pnas.1002436107

Andersen, S. K., Müller, M. M., & Hillyard, S. A. (2011). Tracking the allocation of attention in visual scenes with steady-state evoked potentials. In M. I. Posner (Ed.), *Cognitive neuroscience of attention* (2nd ed., pp. 197–216). Guilford Press. ISBN: 9781609189853.

Desimone, R., & Duncan, J. (1995). Neural mechanisms of selective visual attention. *Annual Review of Neuroscience*, *18*, 193–222. https://doi.org/10.1146/annurev.ne.18.030195.001205

Dodwell, G., Nako, R., & Eimer, M. (2024). The preparatory activation of guidance templates for visual search and of target templates in non-search tasks. *Journal of Cognition*, *7*(1). https://doi.org/10.5334/joc.341

Duncan, J. (2006). EPS mid-career award 2004: Brain mechanisms of attention. *Quarterly Journal of Experimental Psychology*, *59*, 2–27. https://doi.org/10.1080/174702105002606

Duncan, J., & Humphreys, G. W. (1989). Visual search and stimulus similarity. *Psychological Review*, *96*, 433–458. https://doi.org/10.1037/0033-295X.96.3.433

Eimer, M. (1996). The N2pc component as an indicator of attentional selectivity. *Electroencephalography and Clinical Neurophysiology*, *99*, 225–234. https://doi.org/10.1016/0013-4694(96)95711-9

Eimer, M. (2014). The neural basis of attentional control in visual search. *Trends in Cognitive Sciences*, *18*, 526–535. https://doi.org/10.1016/j.tics.2014.05.005

Eimer, M., & Grubert, A. (2014). The gradual emergence of spatially selective target processing in visual search: From feature-specific to object-based attentional control. *Journal of Experimental Psychology: Human Perception and Performance*, *40*(5), 1819–1831. https://doi.org/10.1037/a0037387

Eimer, M., & Kiss, M. (2008). Involuntary attentional capture is determined by task set: Evidence from event-related brain potentials. *Journal of Cognitive Neuroscience*, *20*(8), 1423–1433. https://doi.org/10.1162/jocn.2008.20099

Faul, F., Erdfelder, E., Lang, A. G., & Buchner, A. (2007). G*power 3: A flexible statistical power analysis program for the social, behavioral, and biomedical sciences. *Behaviour Research Methods*, *39*, 175–191. https://doi.org/10.3758/BF03193146

Folk, C. L., Remington, R. W., & Johnston, J. C. (1992). Involuntary covert orienting is contingent on attentional control settings. *Journal of Experimental Psychology: Human Perception and Performance*, *18*(4), 1030–1044. https://doi.org/10.1037/0096-1523.18.4.1030

Giesbrecht, B., Weissman, D. H., Woldorff, M. G., & Mangun, G. R. (2006). Pre-target activity in visual cortex predicts behavioral performance on spatial and feature attention tasks. *Brain Research*, *1080*(1), 63–72. https://doi.org/10.1016/j.brainres.2005.09.068

Grubert, A., & Eimer, M. (2018). The time course of target template activation processes during preparation for visual search. *Journal of Neuroscience*, *38*, 9527–9539. https://doi.org/10.1523/JNEUROSCI.0409-18.2018

Grubert, A., & Eimer, M. (2019). Concurrent attentional template activation during preparation for multiple-colour search. *Journal of Vision*, *19*(10), 233. https://doi.org/10.1167/19.10.233

Grubert, A., & Eimer, M. (2020). Preparatory Template Activation during Search for Alternating Targets. *Journal of Cognitive Neuroscience*, *32*(8), 1525–1535. https://doi.org/10.1162/jocn_a_01565

Huynh Cong, S., & Kerzel, D. (2021). Allocation of resources in working memory: Theoretical and empirical implications for visual search. *Psychonomic Bulletin & Review*, *28*, 1093–1111. https://doi.org/10.3758/s13423-021-01881-5

Luck, S. J., & Hillyard, S. A. (1994). Spatial filtering during visual search: Evidence from human electrophysiology. *Journal of Experimental Psychology: Human Perception and Performance*, *20*, 1000–1014. https://doi.org/10.1037/0096-1523.20.5.1000

Maris, E., & Oostenveld, R. (2007). Nonparametric statistical testing of EEG-and MEG-data. *Journal of Neuroscience Methods*, *164*, 177–190. https://doi.org/10.1016/j.jneumeth.2007.03.024

Ort, E., & Olivers, C. N. L. (2020). The capacity of multiple-target search. *Visual Cognition*, *28*(5–8), 330–355. https://doi.org/10.1080/13506285.2020.1772430

14698986, 2024, 8, Downloaded from https://onlinelibrary.wiley.com/doi/10.1111/psyp.14582 by Test, Wiley Online Library on [08/07/2024]. See the Terms and Conditions (https://onlinelibrary.wiley.com/terms-and-conditions) on Wiley Online Library for rules of use; OA articles are governed by the applicable Creative Commons License

Peirce, J. W., Gray, J. R., Simpson, S., MacAskill, M., Höchenberger, R., Sogo, H., Kastman, E., & Lindeløv, J. K. (2019). PsychoPy2: Experiments in behavior made easy. *Behavior Research Methods*, *51*, 195–203. https://doi.org/10.3758/s13428-018-01193-y

Stokes, M., Thompson, R., Nobre, A. C., & Duncan, J. (2009). Shape-specific preparatory activity mediates attention to targets in human visual cortex. *Proceedings of the National Academy of Sciences*, *106*(46), 19569–19574. https://doi.org/10.1073/pnas.0905306106

Störmer, V. S., & Alvarez, G. A. (2014). Feature-based attention elicits surround suppression in feature space. *Current Biology*, *24*(17), 1985–1988. https://doi.org/10.1016/j.cub.2014.07.030

Wolfe, J. M. (2007). Guided search 4.0: Current progress with a model of visual search. In W. Gray (Ed.), *Integrated models of cognitive systems* (pp. 99–119). Oxford University Press. https://doi.org/10.1093/acprof:oso/9780195189193.003.0008

Wolfe, J. M. (2021). Guided search 6.0: An updated model of visual search. *Psychonomic Bulletin & Review*, *28*, 1060–1092. https://doi.org/10.3758/s13423-020-01859-9

Woodman, G. F., & Luck, S. J. (1999). Electrophysiological measurement of rapid shifts of attention during visual search. *Nature*, *400*, 867–869. https://doi.org/10.1038/23698

SUPPORTING INFORMATION

Additional supporting information can be found online in the Supporting Information section at the end of this article.

Figure S1. 50 ms SOA – Contra/Ipsi Waveforms.

Figure S2. 50 ms SOA – Contra/Ipsi Waveforms – Smoothed.

Figure S3. 100 ms SOA – Contra/Ipsi Waveforms.

Figure S4. 200 ms SOA – Contra/Ipsi Waveforms.

How to cite this article: Dodwell, G., Nako, R., & Eimer, M. (2024). A new method for tracking the preparatory activation of target templates for visual search with high temporal precision. *Psychophysiology*, *61*, e14582. https://doi.org/10.1111/psyp.14582

14698986, 2024, 8, Downloaded from https://onlinelibrary.wiley.com/doi/10.1111/psyp.14582 by Test, Wiley Online Library on [08/07/2024]. See the Terms and Conditions (https://onlinelibrary.wiley.com/terms-and-conditions) on Wiley Online Library for rules of use; OA articles are governed by the applicable Creative Commons License